https://doi.org/10.5194/egusphere-2026-6818
Preprint. Discussion started: 6 November 2026
© Author(s) 2026. CC BY 4.0 License.

Accounting for Microbial–DOC Feedbacks Reveal Ecological Constraints on Artificial Upwelling for Atmospheric Carbon Dioxide Removal

Benjamin Owusu[1], Takasumi Kurahashi-Nakamura[1], Lennard Montag[1], Wolfgang Koeve[2], and Sinikka T. Lennartz[1]

[1]Institute for Chemistry and Biology of the Marine Environment (ICBM), Carl von Ossietzky University Oldenburg, Germany
[2]GEOMAR Helmholtz Centre for Ocean Research Kiel, Kiel, Germany

Correspondence: Benjamin Owusu (benjamin.owusu@uni-oldenburg.de) and Sinikka T. Lennartz (sinikka.lennartz@uni-oldenburg.de)

Abstract. Limiting global warming to 1.5–2 °C has intensified interest in marine carbon dioxide removal (mCDR) to offset residual CO_2 emissions. Artificial upwelling (AU), which pumps nutrient-rich deep waters to the surface to stimulate biological production and enhance carbon export, has primarily been evaluated with respect to particulate organic carbon export. However, the response of dissolved organic carbon (DOC) and its microbial remineralisation remains poorly constrained, although AU has the potential to alter both DOC production and consumption due to nutrient input from subsurface waters. Here, we use an Earth system model with explicit representation of microbial DOC remineralisation to quantify the response of global DOC inventories and air–sea CO_2 fluxes to AU. We perform global simulations in which artificial upwelling (AU) differently affects nutrient limitation for phytoplankton and heterotrophic bacteria. Since the role of iron limitation in bacterial DOC uptake is poorly constrained, we explore a full factorial set of ecological scenarios in which AU confers a competitive advantage to phytoplankton, bacteria, both, or neither. AU alters surface DOC inventories by shifting the balance between phytoplankton-DOC production and bacterial-DOC degradation. When phytoplankton compete more strongly for nutrients than heterotrophs, DOC inventories increase; conversely, stronger bacterial competition reduces DOC stocks. These differences are quantitatively significant for regulating air–sea CO_2 uptake under AU. Our results highlight microbial nutrient competition as a key ecologcial control on DOC-mediated carbon storage, underscoring the need to better constrain phytoplankton–bacteria interactions to assess the efficacy of AU as a carbon dioxide removal strategy.

1 Introduction

Ongoing climate change (Adler et al., 2022; Lee et al., 2023) has drawn the attention towards climate intervention strategies (Hurrell et al., 2024; Boyd and Vivian, 2019). Even future scenarios with strong mitigation measures require setting off hard-to-abate residual emissions to obtain the 1.5-degree-goal of the Paris Agreement (Kikstra et al., 2022; Van Vuuren et al., 2026). Carbon dioxide removal (CDR) is therefore increasingly recognised as one of the climate intervention strategies necessary to complement the reduction of CO_2 emissions. Although CDR techniques remain debated in terms of their feasibility, risks, and

https://doi.org/10.5194/egusphere-2026-6818
Preprint. Discussion started: 6 November 2026
© Author(s) 2026. CC BY 4.0 License.

governance, discussions are already underway about their potential to be scaled up in the coming decades (Mace et al., 2021; Holland-Cunz and Baatz, 2025; Honegger et al., 2022). Models play a key role in exploring the effectiveness of such CDR measures, their overall potential, as well as unintended consequences under different ecological conditions, before large scale field trials are attempted.

One of the proposed CDR strategies is marine carbon dioxide removal (mCDR) via artificial upwelling (AU) (Pan et al., 2016; Oschlies et al., 2010). AU involves pumping up nutrient-rich deep waters to the surface ocean with ocean pipes to enhance biological productivity at the surface, with the intended effect of atmospheric CO_2 drawdown. AU is originally devised to boost primary production in nutrient-depleted subtropical gyres, where limited vertical mixing forces phytoplankton to rely on recycled nutrients, keeping productivity and CO_2 fixation rates low (Field et al., 1998). Enhancing primary production at the surface ocean is intended to increase export production from the photic zone into the deep ocean, where remineralisation releases inorganic nutrients and carbon back to the seawater (a process known as the soft tissue pump) (Volk and Hoffert, 1985), finally leading to a net CO_2 transport from the atmosphere to the ocean's interior.

However, several studies have questioned the efficiency of this simplistic view, arguing against its carbon drawdown potential and climate effects (Shepherd et al., 2007; Yool et al., 2009; Oschlies et al., 2010; Keller et al., 2014). For example, pumping up nutrient rich deep waters, which are also high in dissolved inorganic carbon (DIC) (Sarmiento and Gruber, 2006), may lead to a net CO_2 out-gassing even if AU increases export production (Dutreuil et al., 2009). These contrasting outcomes highlight the need to better understand the mechanisms and conditions under which artificial upwelling can achieve a sustained net carbon sequestration, motivating more comprehensive modelling and experimental assessments.

Dissolved organic carbon (DOC) is the largest organic carbon pool in the ocean with $\sim$700 PgC (Hansell, 2009), and the major source of carbon and energy for heterotrophic bacteria (Zweifel et al., 1993). The amount of DOC storage in the water column depends on the balance between DOC production by phytoplankton and the rate at which heterotrophic bacteria remineralise it across depths (Hopkinson Jr and Vallino, 2005), depending on environmental controls such as grazing pressure or nutrient availability (Hale et al., 2017; Owusu et al., 2026; Zakem and Levine, 2019). Taking nutrient-mediated environmental controls on the remineralisation rate into account, Lennartz et al. (2024) showed that the amount of DOC storage may be closely linked to nutrient cycles. This linkage to nutrient concentrations makes AU prone to affect surface DOC inventories and hence its carbon storage potential. Indeed, a mesocosm study by Gomez-Letona et al. (2022) showed that DOC concentrations can temporarily increase under simulated artificial upwelling conditions, and discussed nutrient limitation as a potential factor contributing to this observation. However, a large scale quantification of the effect of AU on DOC has not yet been realised.

A recent AU modelling study by Jürchott et al. (2023) shows that the ocean's CO_2 uptake is highest under the highest CO_2 emission scenario. However, as in most state-of-the-art biogeochemical ocean models, the DOC remineralisation in Jürchott et al. (2023, 2024) is simplified and does not explicitly resolve the dynamics of heterotrophic bacteria as the main consumers, as well as the environmental drivers that govern microbial DOC degradation. A nutrient-driven feedback on DOC would not be captured by these models, and may affect the assessment of AU as an mCDR strategy. An additional key assumption in Jürchott et al. (2023) was that AU supplies iron to the surface ocean, releasing primary producers from iron-limitation. In the biogeochemical part of that model (Keller et al., 2012; Mengis et al., 2020), iron limitation is realised as a scaling factor for

https://doi.org/10.5194/egusphere-2026-6818
Preprint. Discussion started: 6 November 2026
© Author(s) 2026. CC BY 4.0 License.

the maximum growth rate between 0 (maximal iron limitation) and 1 (no iron limitation), so that growth is reduced under low iron concentrations. Since iron concentration was prescribed from static monthly concentration fields, the release from iron limitation at the surface was done by setting the scaling factor to 1 (no iron limitation) at the surface ocean. Unlike for phytoplankton, there is no consensus on the role of iron limitation for heterotrophic bacteria, as studies yield conflicting results (Pham et al., 2022; Church et al., 2000; Baltar et al., 2018). Hence, the impact of iron inputs on bacterial activity at the global scale remains poorly understood, hampering a robust representation of this process in biogeochemical models.

In this study, we evaluate the impact of AU on the DOC inventory, and assess the overall efficacy of AU with respect to the CO_2 flux when explicitly considering DOC dynamics. We hypothesise that AU may enhance primary production as primary producers utilise additional nutrients, leading to an increase in DOC concentrations. On the other hand, bacteria may compete for these additional nutrients with phytoplankton (Sörenson et al., 2020; Grognard et al., 2015), thereby contributing to a reduction in surface DOC concentrations under AU. To test these hypotheses, we use a biogeochemical model which was recently extended to include an explicit formulation of DOC remineralisation by heterotrophic bacteria (Lennartz et al., 2024; Kurahashi-Nakamura et al., 2026). In particular, we simulate the net effect of AU under varying idealised assumptions of nutrient competitive fitness between bacteria and phytoplankton. We aim to (i) quantify the impact of AU on DOC dynamics until the end of this century, (ii) assess how nutrient competition between bacteria and phytoplankton governs carbon storage and (iii) quantify the influence of heterotrophic DOC remineralisation on the potential impact of AU as an mCDR technique. In this study, artificial upwelling is idealised as being applied globally in regions of potential benefit to test the maximum potential of its net carbon effect.

2 Methods and Modelling

2.1 The Earth System Model

We perform simulations with the University of Victoria Earth System Climate Model (UVic ESCM) version 2.10, a 3D Earth system model of intermediate complexity (Weaver et al., 2001; Mengis et al., 2020) with a dynamic coupling of atmosphere, sea-ice, ocean and terrestrial components (see supplements section 1 for detailed description). UVic ESCM has a horizontal spatial resolution of 1.8 degrees in latitude and 3.6 degrees in longitude for all components, with the ocean having 19 vertical levels with 50 m thickness at the surface and up to 590 m in the deep ocean. The model dynamically simulates carbon cycling with dissolved inorganic carbon (DIC) and alkalinity as prognostic tracers and an ocean ecosystem representation that assumes a fixed Redfield ratio stoichiometry (Keller et al., 2012). It also has a simplified $CaCO_3$ counter pump (Schmittner et al., 2008). Iron concentration is prescribed by an iron concentration mask that remains static throughout the simulation (Galbraith et al., 2010) (see supplements section 1.1 for details). To include the effect of iron limitation, the prescribed iron concentration determines a factor between 0 and 1 by which the primary productivity by phytoplankton is multiplied.

https://doi.org/10.5194/egusphere-2026-6818
Preprint. Discussion started: 6 November 2026
© Author(s) 2026. CC BY 4.0 License.

2.2 The Microbial–DOM Model (MICDOC)

The UVic ESCM was coupled with the microbial-substrate interaction model version 2.0 (MICDOCv2.0) in a bidirectional way (Kurahashi-Nakamura et al., 2026) (Figure 1). The MICDOCv2.0 model we used here is an extension of the existing version in Lennartz et al. (2024). The two important modifications are a bidirectional coupling between MICDOC and UVic ESCM in terms of carbon and nutrients, and the addition of a tracer for dissolved organic phosphorus (DOP). We account for the bacterial carbon-to-phosphorus stoichiometry by introducing a prescribed C:P ratio (63:1) for bacterial biomass. In the MICDOC model, bacterial growth (ρ) is limited by the availability of organic and inorganic nutrients following the Liebig law of the minimum by the expression:

$$\rho = \alpha \cdot B \cdot \min(\mu_{DOC}, (\mu_{DOP} + \mu_{DIP})) \quad (1)$$

where α is the maximum growth rate of bacteria biomass (B) and $\min(\mu_{DOC}, (\mu_{DOP} + \mu_{DIP}))$ is the limiting function that determines the actual growth rate. Here, the growth of bacteria is limited by the lowest uptake rate of either DOC or the combined uptake of DOP and PO_4, the latter serving as a placeholder for macro-nutrient limitation in general. Each of the limiting factor μ follows the Monod function corresponding to the respective species. Because bacteria only access a subset of DOC compounds, the effective rate relative to the entire DOC pool appears lower than to the individual labile substrates, consistent with previous analyses of DOC diversity effects on microbial growth (Mentges et al., 2020; Owusu et al., 2026). In the MICDOC implementation used here, DOC production is not prescribed directly as a fraction of net primary production, but is assumed to account for 15% of the non-living organic material generated through the breakdown, mortality, and excretion of organisms. Note that no direct impact of temperature on bacterial uptake rates is considered, and temperature therefore affects DOC dynamics only indirectly through its influence on nutrient supply. The particulate organic carbon (POC) pool represents the particulate component of organic carbon production and is subject to remineralisation, which contributes to the DIC remineralisation pool.

https://doi.org/10.5194/egusphere-2026-6818
Preprint. Discussion started: 6 November 2026
© Author(s) 2026. CC BY 4.0 License.

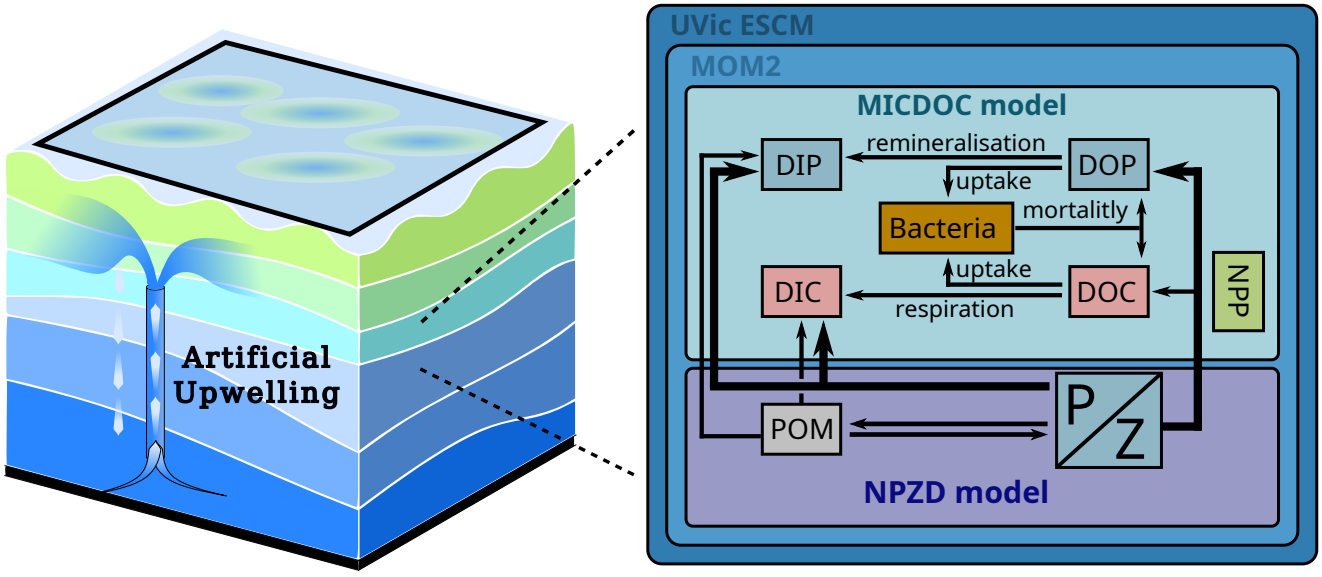


Figure 1. Schematic representation of microbial-substrate interaction version 2.0 (MICDOCv2.0) model, coupled to the UVic ESCM with incorporation of artificial upwelling (AU) that transports deep nutrient rich ocean waters to the surface with a compensating downwelling transport.

2.3 Artificial Upwelling scheme

The AU scheme in this study is based on previous studies with an earlier version of the UVic ESCM (Jürchott et al., 2023; Oschlies et al., 2010). AU is modelled as a water parcel transported adiabatically from the lowest grid cell at the end of a supposed upwelling pipe to the surface grid box at a rate of 1 cm/day averaged over the area of the grid cell. At the same time, a compensating downwelling flux of water from the surface goes through all intermediate levels to ensure volume conservation (Figure 1). Model simulations with the MICDOC framework do not modify the alkalinity budget and do not include any representation of 'organic alkalinity', therefore air–sea inorganic carbon exchange is calculated solely from the inorganic carbonate system (DIC and TA) as implemented in the standard UVic framework. We deploy the pipes only in areas where the sea surface phosphate concentration is lower than 0.4 mmol/m^3 and where a complete uptake of the upwelled macro-nutrients would lead to a reduction in the pCO_2 in the local surface water, in line with Jürchott et al. (2023) (see supplements Figure S9). The location of the pipe is determined during the runtime and we limit the length of the pipes to 1200 m, optimised by the algorithm to maximise for additional local CO_2 uptake (see supplement Figure S9).

2.4 Simulation set-up

The UVic ESCM–MICDOCv2.0 model is initialised with a spun-up pre-industrial state for the conventional UVic ESCM variables (Mengis et al., 2020) and a homogeneous distribution for the MICDOCv2.0 tracers (DOC, DOP and Bacteria). A

https://doi.org/10.5194/egusphere-2026-6818
Preprint. Discussion started: 6 November 2026
© Author(s) 2026. CC BY 4.0 License.

subsequent 10,000 year MICDOC spin-up under constant pre-industrial forcing produced a quasi-steady state for the coupled system. Using this final spun-up state as the initial condition, we performed a transient simulation from 1850 to 2010, which then served as the starting point for each AU run. For the transient simulations, we used an emission driven scenario following the SSP5-8.5 pathway (Gidden et al., 2019), and performed simulations from 2010 to 2110 to assess the potential effectiveness of artificial upwelling.

The model reproduces the large-scale spatial structure and latitudinal gradients of surface nitrate and phosphate, with elevated nutrient concentrations that are pronounced in the Southern Ocean, and lower values in the subtropical gyres (Kurahashi-Nakamura et al., 2026). For model–data comparison, we used the model output for year 2000, averaged over the equivalent of a 20-year climatological period, and compared it against the 1990–2010 climatology from the World Ocean Atlas 2018 (WOA18) (Garcia et al., 2019; Locarnini et al., 2018). Nutrient distributions from this comparison are shown in supplements Section 1.2. The model reproduces the large-scale nutrient distributions but exhibits small systematic biases, including slightly underestimated nutrient concentrations that lead to minor regional deviations in the North Atlantic. For DOC, the model captures the observed latitudinal distribution and magnitude comparable to observational data from Hansell et al. (2021), with minor underestimations in upwelling regions and overestimations in the subtropical gyres and deep ocean.

For the future scenario simulations, we performed one default baseline simulation with the high emission scenario (RCP8.5) which is without AU (referred here as woAU MICDOC). For AU simulations under the same emission scenario, we performed four main simulations in which the relative competitive strength for nutrient uptake between bacteria and phytoplankton is varied. In previous experiments with AU as in Jürchott et al. (2023, 2024), a release from iron limitation upon introduction of iron-rich subsurface waters was realised by alleviating the iron limitation on phytoplankton growth when AU pipes are active. Since there is no consensus on the effect of iron limitation on bacteria (Church et al., 2000; Fourquez et al., 2014; Baltar et al., 2018; Pham et al., 2022), we define four idealised scenarios that explore plausible responses. Our simulations vary in the way the release from iron limitation under AU is treated as: either phytoplankton or bacteria or both receive a growth boost through AU (see Table 1 for full simulation summary). For phytoplankton, following previous approaches, a boost is implemented by setting the iron limitation factor for phytoplankton to 1; meaning phytoplankton growth is no longer reduced by iron limitation. For bacteria, the maximum growth rate is enhanced by 20%. The "NO-BOOST" model version includes the default setting for both so that iron limitation constrains phytoplankton growth even under AU, and bacterial maximum growth rate remains at its default setting. The "P-BOOST" uses the setting in Jürchott et al. (2023) which releases phytoplankton from iron limitation in regions with active AU, but leaves the bacteria unchanged. As such, it mimics a condition in which phytoplankton have been iron limited in the surface ocean before the onset of AU, whereas bacteria were not limited (so that AU does not change their growth). In "B-Boost", bacteria receive a 20% increase in growth rate, consistent with experimental evidence that iron addition can enhance bacteria growth rate by 10-40% in the open ocean (Kirchman et al., 2003; Bertrand et al., 2011; Singh et al., 2015). The simulation "PB-BOOST" then combines the last two. Note that the release of bacteria from iron limitation induced by artificial upwelling is confined to the upper ocean (top three model layers; 0–225 m) and does not extend to deeper layers.

In addition to the five MICDOC model configurations described above, we performed sensitivity analyses based exclusively on

https://doi.org/10.5194/egusphere-2026-6818
Preprint. Discussion started: 6 November 2026
© Author(s) 2026. CC BY 4.0 License.

the NO-Boost configuration, i.e. the model version in which bacterial growth rate is unchanged, and phytoplankton iron uptake remains unchanged (i.e. iron limitation is still in effect). Then, both the bacterial and the phytoplankton growth rates are scaled independently with factors of 0.6, 0.8, 1.0, 1.2, and 1.4 respectively. To test a full factorial design of all combinations, we performed 25 simulations spanning a broad range of relative competitive strengths between phytoplankton and heterotrophic bacteria, while all other model parameters and forcing remained unchanged.

To test the role of microbial-DOC feedbacks, we also perform simulations with and without AU for the original UVic ESCM without MICDOC (i.e., wAU-NO-MICDOC and woAU-NO-MICDOC). Since there are no bacteria present in these model settings, the corresponding simulation with AU is a representative of the "P-Boost" model version. All model code and configuration files, required to reproduce model output from our experiments, are made publicly available at: https://doi.org/10.5281/zenodo.23405565.

To track changes in the DIC inventory attributable to POC remineralisation, we estimated the DIC concentration attributable to POC remineralisation (i.e. $\mathrm{DIC_{remin}}$). Here, we estimated $\mathrm{DIC_{remin}}$ from the apparent oxygen utilisation (AOU), calculated as the difference between oxygen saturation derived from model temperature and salinity and the simulated dissolved oxygen concentration. Using the stoichiometric conversion factor of 0.6625 mol C per mol O_2, $\mathrm{DIC_{remin}}$ was calculated as $0.6625 \times (\mathrm{O_{2,sat}} - \mathrm{O_2})$ and integrated over all ocean grid cells to obtain the global $\mathrm{DIC_{remin}}$ inventory (Garcia and Gordon, 1992).

https://doi.org/10.5194/egusphere-2026-6818
Preprint. Discussion started: 6 November 2026
© Author(s) 2026. CC BY 4.0 License.

Table 1. *Simulation matrix for ecological responses to artificial upwelling (AU). Simulations differ in the inclusion of AU deployment, microbial-DOC (MICDOC) feedback, phytoplankton iron-limitation release, and bacterial iron-limitation release (represented by a 20% increase in bacterial growth rate). The bacterial growth rate increase was applied only when MICDOC feedback was enabled.*

Simulation ID	AU	MICDOC	Phytoplankton Iron-limitation Release	Bacteria Iron-limitation Release
woAU MICDOC *No AU deployment with microbial-DOC interaction*	✗	✓	✗	✗
P Boost *AU releases only phytoplankton from iron limitation*	✓	✓	✓	✗
B Boost *AU releases only bacteria from iron limitation*	✓	✓	✗	✓
PB Boost *AU releases both phytoplankton and bacteria from iron limitation*	✓	✓	✓	✓
NO-Boost *AU releases neither phytoplankton nor bacteria from iron limitation*	✓	✓	✗	✗
AU NO-MICDOC *AU deployment under model framework without microbial-DOC feedback*	✓	✗	✓	N/A
woAU NO-MICDOC *No AU deployment under model framework without microbial-DOC feedback*	✗	✗	✗	N/A

3 Results

3.1 The surface DOC inventory in future scenarios with AU

The DOC inventory in the surface ocean (upper 50 m) is very sensitive to changes in nutrient content and limitation status (Figure 2a). In the default baseline simulation without AU deployment (woAU in Figure 2a), the surface DOC inventory increases to about 15.6 PgC by the end of the simulation. This DOC increase in the climate-perturbed system without AU reflects the projected decline in surface ocean phosphorus concentrations, which is largely driven by enhanced surface stratification under

https://doi.org/10.5194/egusphere-2026-6818
Preprint. Discussion started: 6 November 2026
© Author(s) 2026. CC BY 4.0 License.

changing climate, thereby limiting DOC degradation as described elsewhere (Kurahashi-Nakamura et al., 2026).

In scenarios where AU is deployed, the additional input of nutrients from deeper waters alters DOC storage in the surface ocean through; (i) input of macronutrients (here, impacting both phytoplankton and bacterial growth), (ii) upwelling of cooler water masses (here impacting only phytoplankton in our simulations) and (iii) through input of iron, which we simulate by boosting the maximum growth rates of phytoplankton and bacteria. Depending on the iron limitation status of phytoplankton and bacteria, the DOC inventory either decreases or increases during the simulation period under AU deployment. The differences spanned approximately $\sim$5 PgC across the four ecological scenarios.

The largest increase in the DOC surface inventory occurs when phytoplankton are released from iron limitation, but bacteria do not receive a growth enhancement. This model configuration mimics an ecological condition where bacteria are not primarily iron limited in the present-day ocean (P-Boost). This setting leads to a continuous increase in the surface DOC inventory to about 17.2 PgC, translating to approximately 25% increase relative to its initial inventory at the start of the simulation. This trajectory is in contrast with the B-Boost model version, in which growth of bacteria is enhanced, but phytoplankton remains iron limited. Here, DOC decreases from the start of the simulation (13.8 PgC) until around the year 2060 (12.0 PgC), followed by an increase until the end of the simulation (12.8 PgC). The P-Boost and B-Boost simulations represent contrasting ecological scenarios; the former leading to higher DOC accumulation and the latter leading to higher DOC consumption, compared to the baseline simulation woAU. Together, they illustrate how shifts in the competitive advantage for nutrients between phytoplankton and bacteria can drive DOC responses under AU in opposite directions, depending on how iron limitation regulates their relative competitiveness. In both scenarios where phytoplankton and bacteria are either released from iron limitation (PB-Boost) or neither is released (No-Boost), the surface DOC inventory remains close to but below that of the reference model version without AU (woAU) throughout the simulations, contrasting with the opposing DOC responses observed in the P-Boost and B-Boost simulations.

The temporal change of the DOC inventory is a result of the relative variations of DOC production and consumption. Both NPP (to 115-124 PgC year^{-1}) and DOC production (to 9.0–9.7 PgC year^{-1}) increase significantly in all AU scenarios, compared to the baseline simulation without AU (Figure 2b and d). Similarly, DOC consumption rates via bacterial uptake increase under AU scenarios (7.2-7.6 PgC year^{-1}, Figure 2c) compared to the baseline scenario without AU (5.2 PgC year^{-1}). The resulting DOC inventory is a combination of the two: For example, P-Boost has the second highest production rate increase, but the lowest DOC consumption rate increase due to the boost in maximum growth rate of phytoplankton, hence, the DOC inventory increases strongest. The comparison of the production and consumption rates among the four ecological scenarios shows that AU leads to a faster carbon cycling by increasing both production and consumption rates, but that the difference in the way these rates are impacted crucially determines the resulting carbon storage in DOC.

https://doi.org/10.5194/egusphere-2026-6818
Preprint. Discussion started: 6 November 2026
© Author(s) 2026. CC BY 4.0 License.

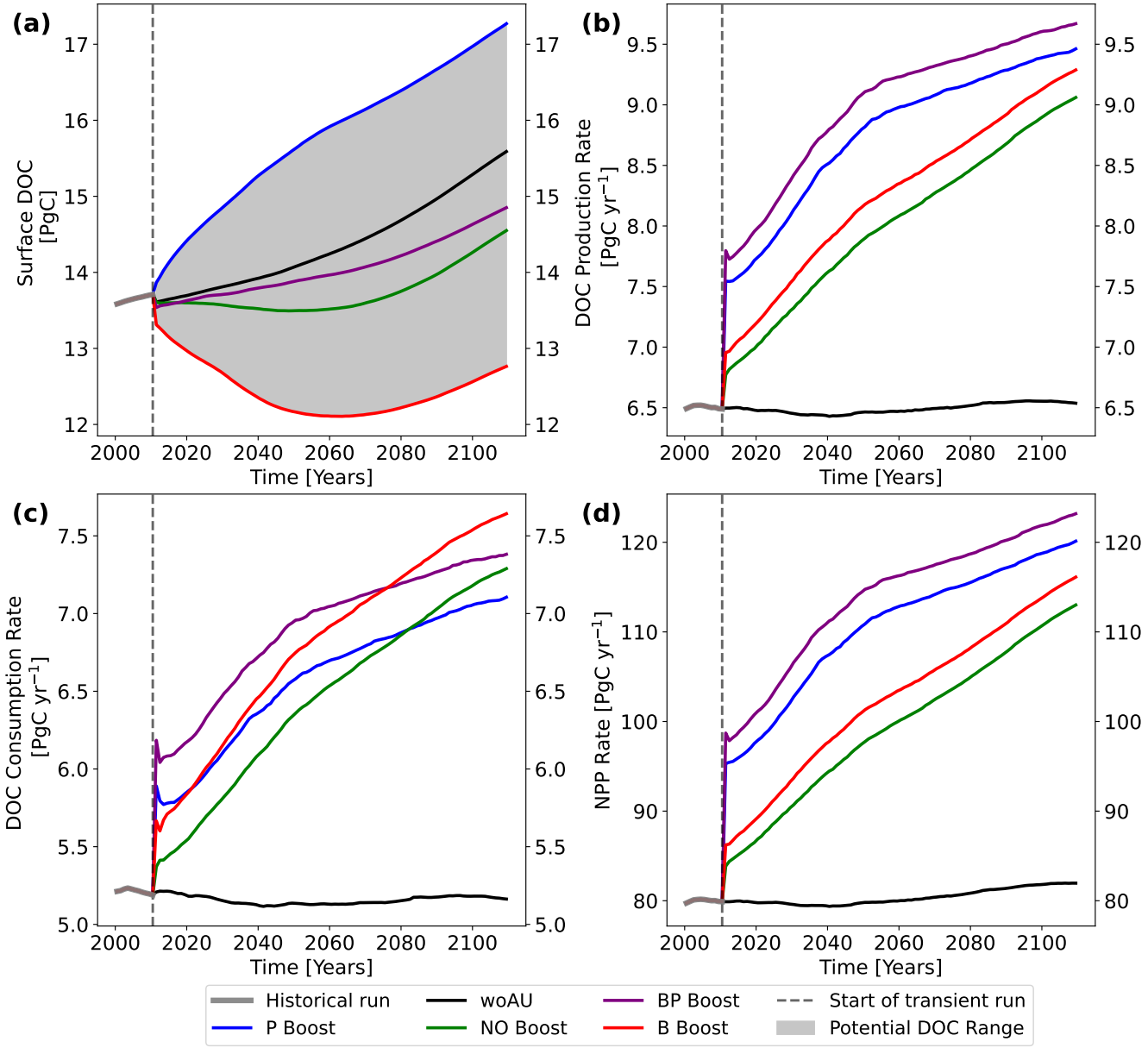


Figure 2. Time series of global surface ocean (upper 50 m) (a) DOC inventory, (b) DOC production, (c) DOC consumption, and (d) net primary production (NPP) rates across the different AU model simulations with colour-coded as shown in legend. The gray solid line denotes the common historical trajectory, shown for the last 20 years preceding the transient simulations. The dashed vertical line marks the start of the transient simulations, beyond which all scenarios diverge from the common historical run. In panel (a), the gray shaded envelope indicates the potential range within which surface DOC inventory may lie under artificial upwelling in response to ecological changes, across model configurations.

https://doi.org/10.5194/egusphere-2026-6818
Preprint. Discussion started: 6 November 2026
© Author(s) 2026. CC BY 4.0 License.

DOC production and consumption show different sensitivities towards the maximum growth rates of phytoplankton and bacteria, making the resulting net DOC accumulation a function of both parameters (Figure 3). Across the sensitivity simulations, changes in maximum bacterial growth rates had a stronger effect on DOC storage than changes in phytoplankton growth rates, as indicated by the steeper slopes of the bacterial isolines (dot-dashed lines in Figure 3) compared with the phytoplankton isolines (dotted lines). Enhanced bacterial growth increases DOC remineralisation, thereby reducing DOC retention in the surface ocean. These results indicate that bacterial remineralisation exerts a stronger control on long-term DOC storage than enhanced phytoplankton growth.

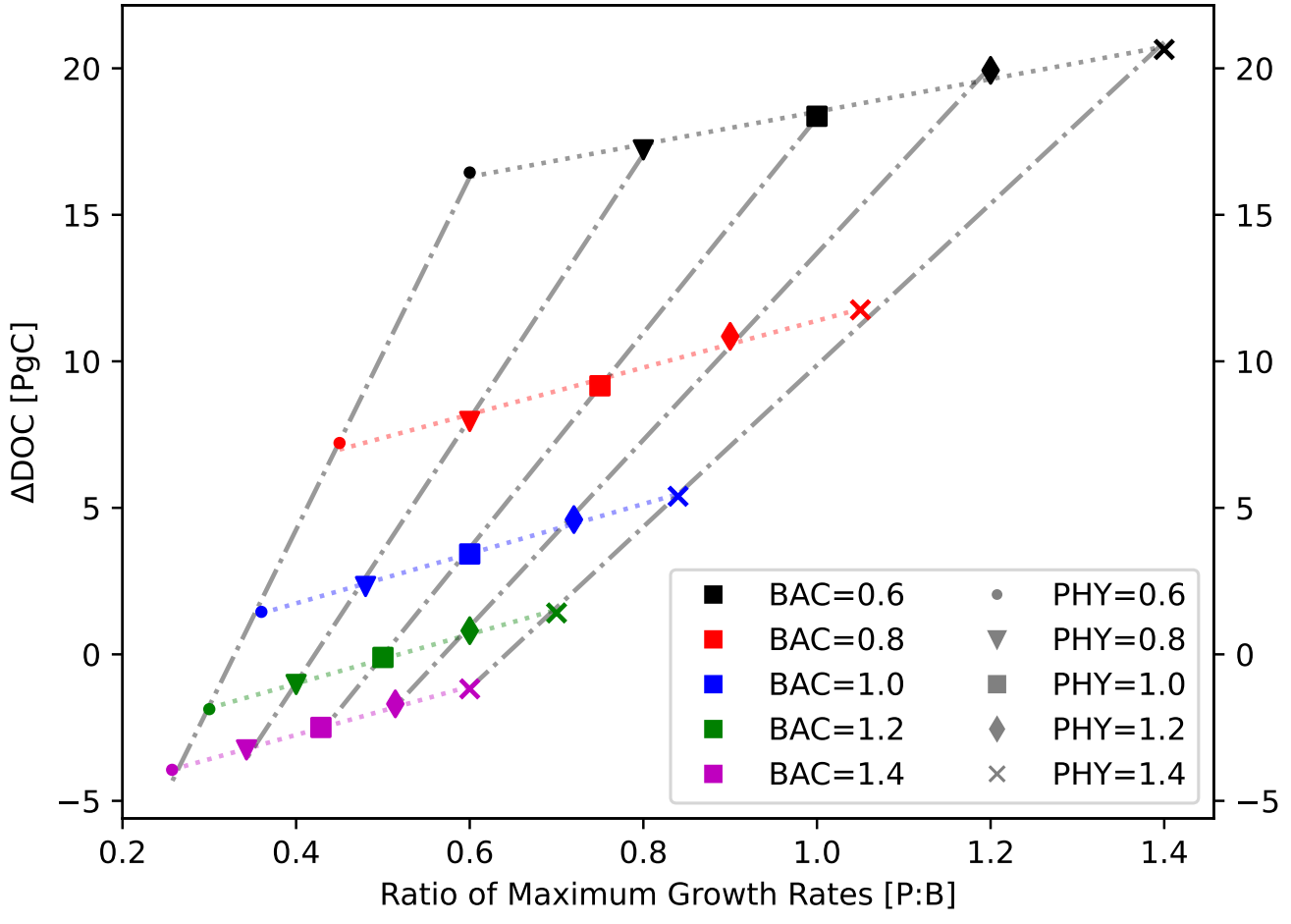


Figure 3. Difference in the inventory size of the global surface (upper 50 m) DOC pool between start and end of each transient simulations [PgC] for different competitive fitness between phytoplankton and heterotrophic bacteria. The ratio of maximum growth rate [P:B] on the x-axis is calculated from the applied factor for phytoplankton divided by the factor for bacteria. Dashed and dotted lines are shown for linear regressions, grouped for bacterial or phytoplankton uptake factors (all reached 99%-significance level).

https://doi.org/10.5194/egusphere-2026-6818
Preprint. Discussion started: 6 November 2026
© Author(s) 2026. CC BY 4.0 License.

3.2 Impact of AU on carbon stocks and fluxes under explicit consideration of heterotrophic DOC remineralisation

Artificial upwelling influences DIC and DOC stocks in the surface (upper 50 m) and global ocean, leading to substantial changes in both inventories depending on the ecological scenario considered (Figure 4, see supplements Table S1 for other tracer-specific carbon stocks). The simulations in which only phytoplankton are released from iron limitation (P-Boost) shows the strongest increase in surface and global DOC inventories (+1.68 and +13.93 PgC respectively, relative to the baseline simulation; Figure 4a,b). The contrasting simulation in which only maximum bacterial growth rate is enhanced shows a decline in surface and global DOC inventories of about -2.83 and -21.92 PgC respectively (Figure 4a,b).

However, the ecological scenario considered does not affect DOC alone, but also triggers changes in other carbon inventories, including DIC, which is in direct exchange with atmospheric CO_2. AU does not only affect the concentration of DIC through altered remineralisation of DOC, but also affects export production. As such, the global inventory of DIC is affected by altered rates of POC remineralisation, as shown by anomalies in the DICremin inventories (supplement Figure S18). In ecological scenarios P-Boost and PB-Boost, when primary production is enhanced, the DICremin inventory increases by approximately 18 and 21 PgC respectively compared to the baseline scenario by 2100. In contrast, a reduction of primary production in NO-Boost and B-Boost scenarios lead to a reduction of the DICremin inventory by approximately -22 and -25 PgC respectively respectively compared to the baseline simulation by 2100.

The differing ranking of changes in DOC and DIC inventories between the surface and global inventories (Figure 4) suggests that large-scale carbon transport processes exert depth-dependent influences on their distribution. The surface-ocean DIC inventories increase in both B-Boost and NO-Boost model variants (+0.85 and +1.21 PgC respectively) while it decreases in both P-Boost and PB-Boost (-0.59 and -0.84 PgC). For the entire ocean, the DIC inventories increases across all model variants. While the ranking of DOC inventories among the four MICDOC model variants under AU are qualitatively similar at the surface (Figure 4a) and in the entire ocean (Figure 4b) (P-Boost > PB-Boost > NO-Boost > B-Boost), there are clear differences seen in the spatial patterns of the surface and global DIC inventories (Figure 4a and b). These differences may be attributed to large-scale carbon transport into the deep ocean. The surface and global DOC responses further suggest that DOC produced or retained near the surface is redistributed and/or remineralised along ocean circulation pathways, contributing to differences in the partitioning and export of carbon within the ocean among the four scenarios (see supplements Figures S16 and S17). In scenarios with enhanced surface DOC accumulation, a fraction of this organic carbon is transported away from the production regions into the ocean interior before being remineralised, whereas enhanced bacterial activity promotes more rapid conversion of DOC back to DIC during transport. Consequently, the contrasting surface DOC responses are accompanied by substantially larger changes in global DOC inventories, indicating that DOC produced or retained near the surface is redistributed into the ocean interior, where it can be transported along circulation pathways and subsequently remineralised. Together, these global anomalies in carbon inventories accumulate to changes in the oceanic carbon uptake across the simulations relative to the baseline (Figure 4c), i.e. the changes in DOC and DIC inventories add up to the cumulative carbon uptake (P-Boost (81.84 PgC) > PB-Boost (62.18 PgC) > NO-Boost (8.93 PgC) > B-Boost (-4.95 PgC)). The change in other carbon inventories such as biomass only marginally impacts CO_2 fluxes (supplements, Table S1).

https://doi.org/10.5194/egusphere-2026-6818
Preprint. Discussion started: 6 November 2026
© Author(s) 2026. CC BY 4.0 License.

Air–sea CO_2 flux is controlled by the difference in pCO_2 between the surface ocean and atmosphere (Figure 4c). The anomaly in surface ocean pCO_2 decreases across all AU simulations (Figure 4d), indicating an increased CO_2 uptake relative to the baseline scenario without AU. However, the magnitude of the decrease in pCO_2 differs among ecological model variants. The strongest reduction in pCO_2 occurs in P-Boost, whereas B-Boost and NO-Boost show smaller pCO_2 reductions. The DOC anomalies show a slightly different picture; here, the largest increase occurs in the P-Boost scenarios, but the lowest anomaly is the B-Boost scenario. Again, this indicates that the response of surface pCO_2 is not determined by DOC alone. Instead, our simulations show that the net effect in pCO_2 results mainly from changes to the DOC and DIC inventories, mediated through the physical transport and the remineralisation of both POC and DOC.

https://doi.org/10.5194/egusphere-2026-6818
Preprint. Discussion started: 6 November 2026
© Author(s) 2026. CC BY 4.0 License.

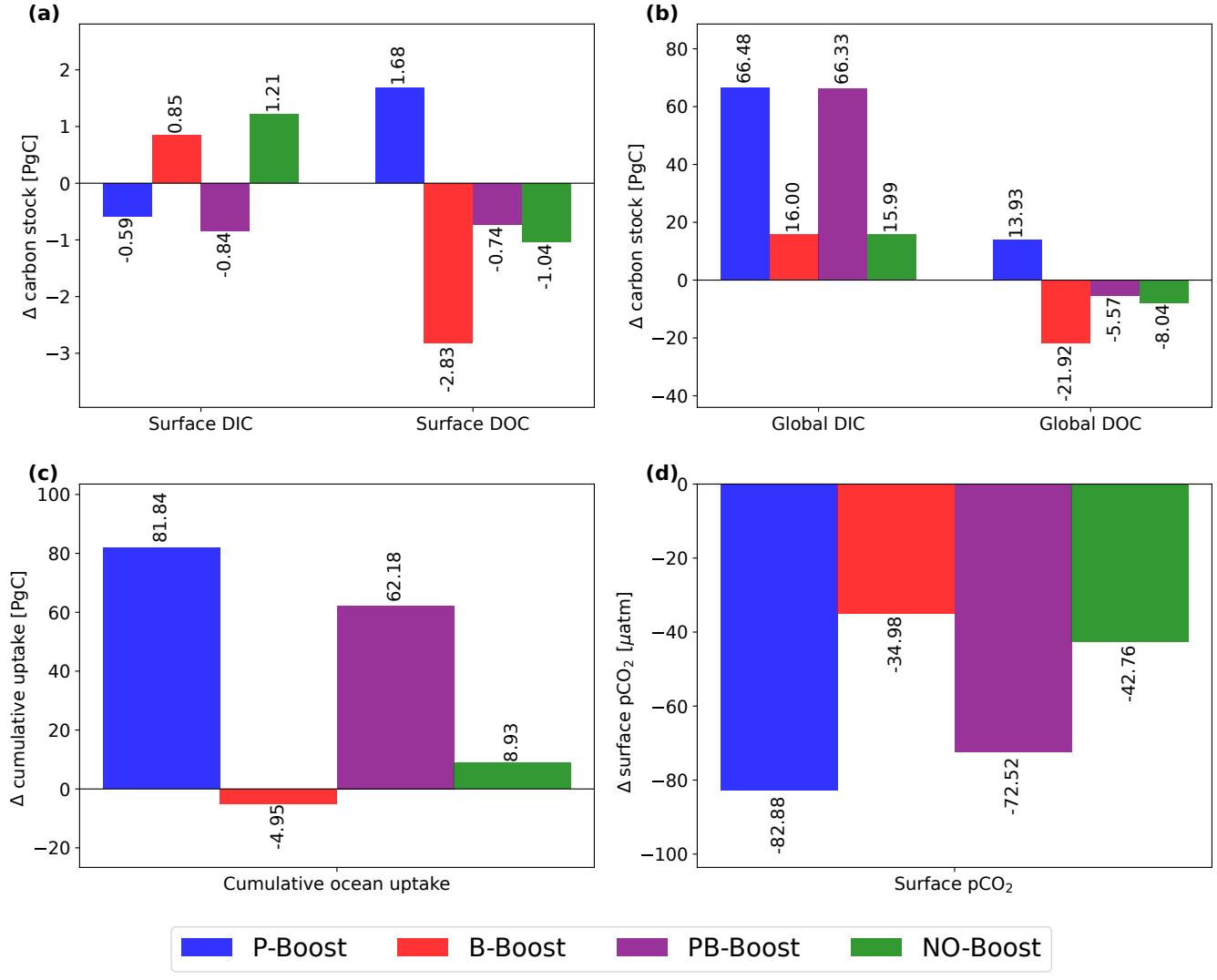


Figure 4. Anomalies relative to the baseline MICDOC simulations without AU (i.e., AU simulations - woAU) for (a) surface (upper 50 m) DIC and DOC inventories [PgC] at the end of the simulation year 2110, (b) global DIC and DOC inventories [PgC] at the end of the simulation year 2110, (c) cumulative air-sea CO_2 flux with positive downward across the full simulation period (100 years) and (d) surface ocean pCO_2, at the end of the simulation year 2110. The air-sea CO_2 flux represents the total carbon input into the ocean over the simulation period, calculated by integrating surface CO_2 fluxes over time and space, and expressed relative to the baseline simulation. Thus, all values shown represent differences relative to the woAU simulation. Positive anomalies indicate enhanced ocean carbon uptake relative to the woAU simulation, while negative values indicate reduced uptake. The different simulated model versions correspond to their respective colour-code in the legend.

https://doi.org/10.5194/egusphere-2026-6818
Preprint. Discussion started: 6 November 2026
© Author(s) 2026. CC BY 4.0 License.

3.3 Atmospheric-ocean carbon flux in AU scenarios with and without explicit consideration of heterotrophic DOC remineralisation

In the historical simulations, where AU is not activated, air-sea CO_2 flux increases steadily towards the branching year (2010). Following the activation of AU, all simulations show a further increase in CO_2 flux until approximately 2080, after which the flux levels off and gradually declines towards the end of the century (Figure 5). Despite these qualitatively similar temporal trajectories, quantitative differences emerge between the model versions with and without explicit consideration of heterotrophic DOC remineralisation (MICDOC and NO MICDOC). In the MICDOC baseline simulation without AU (black curve), the absolute CO_2 flux reaches about 6.2 PgC (Figure 5a), whereas in the corresponding NO MICDOC simulation (pink curve) it increases to about 6.5 PgC year^{-1} before gradually declining. Thus, the explicit consideration of heterotrophic DOC remineralisation results in a lower absolute CO_2 uptake, with an offset of about 0.3 PgC year^{-1} between the two model versions.

Within the MICDOC simulations, the different ecological controls on nutrient limitation introduce an additional range of approximately 1 PgC year^{-1} CO_2 fluxes under AU (Figure 5a). This spread is generally smaller than the dominant increase in CO_2 uptake associated with global warming, but remains quantitatively discernible throughout the simulations. The NO MICDOC simulation show an increase of about 1.5 PgC year^{-1} with AU, but does not include the associated ecological controls on bacterial and phytoplankton nutrient limitation. The largest absolute CO_2 flux occurs in the NO MICDOC simulation with AU reaching approximately 8 PgC year^{-1} by 2110 (Figure 5a), the smallest in the simulation without AU with explicit remineralisation (MICDOC). Comparing the NO MICDOC simulations with their corresponding MICDOC scenario (P-Boost) shows that under comparable conditions when phytoplankton is relieved from iron limitation, NO MICDOC simulations consistently exhibits a higher CO_2 flux than the corresponding MICDOC scenario, both with and without AU.

The relative increase in CO_2 flux allows for a comparison that accounts for the different starting conditions of MICDOC and NO-MICDOC for the AU simulations in year 2010. The relative increase in CO_2 flux in the NO MICDOC simulation lies within the range of responses obtained across the four MICDOC ecological scenarios, falling approximately in the middle of this range (Figure 5b). In the NO MICDOC simulations, the relative CO_2 flux increases by approximately 170%, compared to about 130% in the corresponding simulation without AU (Figure 5b) by 2110. With MICDOC, the relative increase spans approximately 160-200% across the ecological scenarios, compared to a baseline increase of about 150% without AU (Figure 5b). Summed over the duration of one hundred years of the simulation, the NO-MICDOC configuration produces 64.81 PgC of additional cumulative ocean CO_2 uptake relative to woAU; a value that lies within the -4.95 to 81.84 PgC range across the MICDOC ecological scenarios (Supplementary Figure S20).

https://doi.org/10.5194/egusphere-2026-6818
Preprint. Discussion started: 6 November 2026
© Author(s) 2026. CC BY 4.0 License.

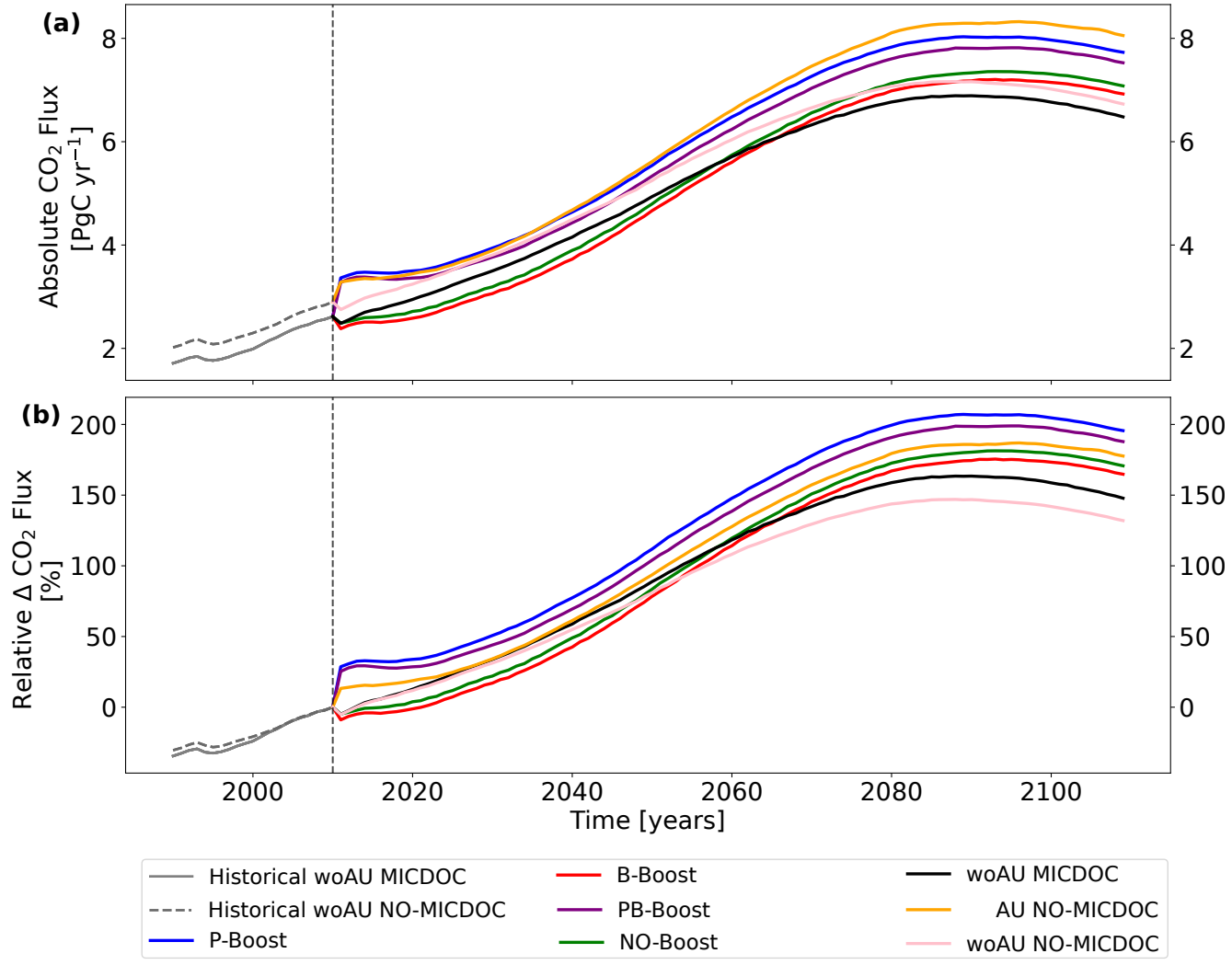


Figure 5. Temporal evolution of CO_2 flux across MICDOC and NO-MICDOC simulations with and without artificial upwelling (AU). Panel (a) shows the absolute CO_2 flux [PgC year^{-1}] across model simulations for both MICDOC and NO-MICDOC configurations, while panel (b) shows the corresponding relative changes in global air-sea CO_2 flux referenced to the last time step of the historical branch-year in 2010 (i.e. just before AU is switched on). The relative changes in CO_2 flux were calculated as $\frac{F(t)-F(hist_{2010})}{F(hist_{2010})} \times 100$, where $F(hist_{2010})$ is the flux at the branching year for the corresponding historical run and $F(t)$ is the total, globally integrated air-sea CO_2 flux at time t. The historical CO_2 fluxes for both MICDOC and NO-MICDOC show the last two simulation decades without AU deployment, while the coloured curves show the trajectories of each model version as shown in the legend. The gray vertical dashed lines indicate the starting year of the transient model runs.

https://doi.org/10.5194/egusphere-2026-6818
Preprint. Discussion started: 6 November 2026
© Author(s) 2026. CC BY 4.0 License.

4 Discussions

4.1 The size of the DOC inventory in AU scenarios

Net changes in the surface DOC inventory under artificial upwelling are influenced by the balance between DOC production and microbial consumption. Across all four AU model configurations, both DOC production and microbial DOC consumption increase relative to the woAU simulation due to the nutrient input that enhances primary production. However, because these two processes do not increase by the same magnitude, the resulting DOC inventory can either increase or decrease depending on the ecological configuration. If enhanced DOC production exceeds microbial consumption, surface DOC will accumulate, whereas stronger bacterial consumption and remineralisation reduce surface DOC retention. Such changes in DOC inventories following artificial upwelling events have been shown in mesocosm experiments, which showed that nutrient enrichment can stimulate DOC production during phytoplankton blooms, while the persistence of this DOC depends on its subsequent microbial utilisation (Gomez-Letona et al., 2022).

The sensitivity of DOC accumulation to varying ratios of phytoplankton and bacterial maximum growth rates as demonstrated by sensitivity tests (Figure 3) shows that changes in the phytoplankton maximum growth rate altered the DOC inventory by approximately 5 PgC, whereas comparable changes in the bacterial maximum growth rate produced a response of approximately 20 PgC in 100 years. This difference indicates a substantially greater sensitivity of DOC accumulation to bacterial growth capacity. This relative competitive strength of phytoplankton and bacteria is therefore an important control on the direction and magnitude of DOC accumulation under AU. Experimental evidence shows that heterotrophic bacteria can compete strongly with phytoplankton for inorganic nutrients (Joint et al., 2002; Danovaro, 1998; Currie and Kalff, 1984). In particular, mesocosm experiments have demonstrated that enhanced bacterial activity can suppress phytoplankton through competition for available inorganic nutrients (Joint et al., 2002), while experimental and theoretical studies have shown that bacteria can acquire inorganic nutrients at a level to compete with phytoplankton for phosphorus (Danovaro, 1998; Currie and Kalff, 1984). The strong DOC sensitivity to bacterial growth in our simulations is consistent with the potential for heterotrophic bacteria to exert substantial control over nutrient availability and carbon partitioning under AU.

The likelihood that a particular ecological response represented by our simulated model variants may occur in real oceans under artificial upwelling depends on the local nutrient-limitation regime and on how phytoplankton and heterotrophic bacteria respond to the nutrients supplied by artificially upwelled nutrient-rich waters. In particular, the B-Boost configuration, in which bacteria are released from iron limitation while phytoplankton remain iron-limited, is likely to represent a less probable response in regions where phytoplankton growth is already known to be strongly iron-limited. Observational and modelling studies demonstrate widespread phytoplankton iron limitation, particularly in high-nutrient, low-chlorophyll (HNLC) regions, where an increased supply of bioavailable iron can stimulate phytoplankton growth (Behrenfeld et al., 1996; Bertrand et al., 2011; Geider and La Roche, 1994). In contrast, there is no consensus on whether bacteria are iron limited in major parts of the ocean or not (Pham et al., 2022; Church et al., 2000; Baltar et al., 2018; Mellett et al., 2026). Still, the likelihood of a scenario in which only bacteria are iron limited in the present-day ocean, and released from iron limitation upon onset of AU (B-Boost) is the least likely scenario because of the widespread evidence for iron limited phytoplankton. Nevertheless, the magnitude and

https://doi.org/10.5194/egusphere-2026-6818
Preprint. Discussion started: 6 November 2026
© Author(s) 2026. CC BY 4.0 License.

even direction of the resulting DOC response will depend on the local limitation status of both groups, and therefore may vary spatially across the ocean. The P-Boost and PB-Boost model versions may reflect conditions under which phytoplankton gains a growth advantage when iron limitation is relieved, either alone or alongside bacterial stimulation (Bertrand et al., 2011). In contrast, the NO-Boost simulation may closely represent a likely ecological response, in which artificial upwelling does not substantially alleviate iron limitation for either phytoplankton or heterotrophic bacteria, resulting in a modest decline in the global DOC inventory. Such a scenario is likely under the assumption that iron remineralised in the deep sea is rapidly scavenged by sinking particles (Jürchott et al., 2024; Parekh et al., 2004).

Taken together, our model simulations should be interpreted as the range of idealised ecological responses to artificial upwelling rather than as definitive predictions. Our experiments serve as an illustration to how differences in the relative competitive strength of phytoplankton and heterotrophic bacteria substantially influence DOC concentrations under identical AU forcing. They establish the important role of explicitly resolving remineralisation processes, which could react more sensitively to nutrient input than DOC production, affecting the efficacy of artificial upwelling as a carbon-removal strategy.

4.2 Implications of DOC dynamics on the global CO_2 flux in AU scenarios

The effects of surface DOC dynamics under artificial upwelling is not limited to DOC alone, as changes in surface DOC production and microbial consumption significantly shift the partitioning of carbon between organic and inorganic pools (Jiao and Azam, 2011). In our AU simulations, the P-Boost experiment exhibits both the largest surface DOC accumulation and the largest cumulative air-sea CO_2 uptake, suggesting that enhanced retention of carbon as DOC may contribute to increased ocean carbon storage. However, the differences in cumulative CO_2 uptake among the model configurations cannot be solely attributed to changes in surface DOC, as illustrated by the positive cumulative uptake anomaly in the NO-Boost simulation despite its reduced DOC inventory (Figure 4). Thus, changes in surface DOC need to be considered together with their effects on the DIC pool and subsequent carbon transport and remineralisation.

The surface DOC dynamics also influence the inorganic carbon reservoir through microbial remineralisation and physical transport. Microbial degradation of DOC transfers organic carbon back to the inorganic carbon pool, while ocean circulation redistributes both DOC and DIC away from the surface and into the ocean interior (Lévy et al., 2013; Hansell and Carlson, 2001). The contrasting surface and global DIC responses in our simulations indicate that carbon is redistributed from the surface to the ocean interior, with global DIC inventories increasing across all four AU simulations (see supplements Figures S18 and S19). Differences in DIC_{remin} among the ecological scenarios reflect differences in the production and subsequent remineralisation of POC, which are influenced indirectly by the microbial processing of DOC through changes in nutrient recycling and primary production. Together, these results show that DOC dynamics influence not only the size of the surface DOC pool but also the transfer and retention of carbon between organic and inorganic reservoirs throughout the ocean.

These combined changes in DOC and DIC influence surface pCO_2 and, consequently, the air–sea CO_2 flux. Microbial degradation of DOC transfers organic carbon back to the inorganic carbon pool, potentially increasing surface pCO_2 and thereby weakening oceanic CO_2 uptake (Azam et al., 1994). The strongest reduction in surface pCO_2 occurs in the P-Boost simulation, which also exhibits the largest increase in surface DOC, consistent with enhanced retention of carbon in the DOC pool (Fig-

https://doi.org/10.5194/egusphere-2026-6818
Preprint. Discussion started: 6 November 2026
© Author(s) 2026. CC BY 4.0 License.

ure 4). However, the positive cumulative CO_2 uptake in the NO-Boost simulation despite its reduced DOC inventory shows that the integrated air–sea CO_2 response is not determined by surface DOC accumulation alone. Instead, it reflects the combined effects of carbon partitioning between DOC and DIC, microbial remineralisation, and the physical redistribution of carbon within the ocean. In particular, physical processes associated with artificial upwelling can redistribute DIC and carbon into the ocean interior, contributing to CO_2 uptake even when changes in surface DOC or DIC remineralisation are small or negative (Jürchott et al., 2023; Yool et al., 2009; Oschlies et al., 2010). Thus, the cumulative air-sea CO_2 flux integrates the effects of biological carbon processing and physical carbon transport rather than representing a direct measure of DOC accumulation alone.

The magnitude of the simulated CO_2 uptake also places the potential contribution of artificial upwelling into perspective. The P-Boost simulation, representing the largest DOC accumulation and cumulative air–sea CO_2 uptake among our ecological scenarios, yields a time-averaged additional carbon removal of approximately 0.82 PgC year^{-1} over the 100-year simulation period. This corresponds to only about 7 % of the current anthropogenic CO_2 emissions ($\sim$11 PgC year^{-1}) and remains below the $\sim$4 PgC year^{-1} of hard-to-abate residual emissions projected under stringent mitigation pathways (Friedlingstein et al., 2024). This estimate should nevertheless be interpreted as an idealised upper-bound sensitivity rather than a deployment-level projection, because the simulations are forced by the high-emission SSP5-8.5 scenario. Under this scenario, the sustained increase in atmospheric CO_2 strengthens the atmosphere–ocean CO_2 gradient and thereby enhances the physically mediated component of AU-induced uptake. Under mitigation pathways, slower atmospheric CO_2 growth would reduce this gradient and consequently diminish this component of the uptake (Jürchott et al., 2023). Thus, even the idealised upper-bound carbon-removal rate from our P-Boost model version is likely an upper limit.

4.3 Efficacy of AU under explicit consideration of heterotrophic DOC remineralisation

Under artificial upwelling, additional nutrient availability stimulates not only primary production and DOC formation but also bacterial processing of the resulting organic carbon (Gomez-Letona et al., 2022; Hao et al., 2026). Microbial stoichiometry and co-limitation (DOC, organic and inorganic macronutrients) determine growth yields and govern whether bacteria are carbon or macronutrient limited (Owusu et al., 2026; Lennartz et al., 2024). Without an explicit microbial (co-)limitation mechanism as implemented in our microbial-DOC (MICDOC v2.0) model, modelled artificial upwelling scenarios miss how additional nutrient input shifts the balance between DOC production and consumption and hence, DOC net accumulation (Polimene et al., 2006; Tang and Riley, 2021; Lennartz et al., 2024). Particularly, the enhanced DOC production associated with nutrient enrichment may be retained more strongly than in a system where bacterial remineralisation responds dynamically to the same nutrient perturbation, potentially leading to an overestimation of the associated CO_2-uptake response. Our study extended approaches by Jürchott et al. (2023, 2024) and Yool et al. (2009) with the heterotrophic impact. The study by Jürchott et al. (2023) is directly comparable to our NO-MICDOC simulations.

The relative increase in CO_2 flux with and without the explicit consideration of heterotrophic remineralisation shows that AU enhances CO_2 fluxes in both model versions. However, similar to the findings about the ecological scenarios affecting the DOC pool, a similar pattern emerges for the CO_2 flux. Not considering the effect of heterotrophic microbes places the additional

https://doi.org/10.5194/egusphere-2026-6818
Preprint. Discussion started: 6 November 2026
© Author(s) 2026. CC BY 4.0 License.

CO_2 uptake by the ocean between the ecological scenarios in which remineralisation is explicitly included (MICDOC). This range demonstrates that the simulated CO_2 uptake response to AU depends on the underlying ecological controls on nutrient limitation. Relative to the woAU MICDOC baseline, these values correspond to an additional increase of approximately 7–33% in global CO_2 flux by 2110.

Consistent with the findings about DOC discussed above, also the overall CO_2 flux is quantitatively impacted by the different ecological scenarios, highlighting the role of microbial remineralisation in regulating carbon cycling and the air-sea CO_2 response to artificial upwelling. Without accounting for explicit remineralisation and the corresponding nutrient competition between phytoplankton and bacteria can therefore lead to overestimations of the true CO_2 uptake. This overestimation is negligible if AU only relieves phytoplankton from iron limitation (P-Boost), but quantitatively significant if none or only bacteria are substantially relieved from iron limitation (B-Boost or NO-Boost). Jürchott et al. (2024) indicates that iron scavenging in the deep ocean might reduce the effect of iron introduced to the surface water on phytoplankton growth, pointing towards the latter scenarios being more likely.

Bacterial uptake and remineralisation of DOC provide an additional pathway for carbon transformation and nutrient recycling, thereby modifying the balance between DOC accumulation, remineralisation, primary production, and DIC. Consequently, explicitly resolving microbial–DOC feedbacks is important when assessing the efficacy of artificial upwelling as a carbon removal strategy.

5 Conclusions

Artificial upwelling (AU) has gained recognition as a marine carbon dioxide removal strategy to enhance ocean carbon uptake by supplying nutrient-rich deep waters to the surface to reinforce the biological pump. Model studies are essential tools to test its feasibility before large scale deployment. From this study, there are three major implications for the efficacy of artificial upwelling in a future high-emission scenario.

First, the balance between DOC production and consumption under artificial upwelling is controlled by the relative competitive ability of phytoplankton and heterotrophic bacteria for nutrient uptake. In our case, this was tested with a focus on iron limitation, but in general it may apply to any nutrient that limits the growth of either or both of the heterotrophic and the autotrophic communities. While AU increases production of organic matter, the additional nutrient input also enhances its degradation. Our results highlight that the net effect critically depends on the competition for limiting nutrients between phytoplankton and bacteria, indicating a strong ecological control that has not been previously considered in AU assessments.

As a second finding, the simulations show that this effect is quantitatively significant not only for the surface DOC inventory, but also for the additional CO_2 flux attributable to artificial upwelling. Across our simulations, the additional air–sea CO_2 uptake varies depending on the ecological conditions of our model simulation. This spread illustrates that the nutrient limitation status of phytoplankton and heterotrophic bacteria; specifically whether iron limitation is alleviated in either or both, determines whether artificial upwelling enhances or diminishes net CO_2 sequestration. As such, AU's effectiveness depends critically on the "present-day" ecological state of nutrient limitation in the ocean, which are only poorly understood. Under-

https://doi.org/10.5194/egusphere-2026-6818
Preprint. Discussion started: 6 November 2026
© Author(s) 2026. CC BY 4.0 License.

standing the limiting factors for phytoplankton and bacterial growth is therefore crucial.

Finally, simulations without microbial–DOC feedback may misrepresent the efficacy of artificial upwelling by ignoring nutrient-driven microbial remineralisation pathways and the effect of nutrient recycling on primary production. Not accounting for the effect of altered bacterial remineralisation during AU can overestimate the absolute CO_2 flux. The flux enhancement expected from AU may be smaller than expected, because additional nutrient input does not only affect biological production by phytoplankton, but also increase remineralisation and hence, reduce the CO_2 uptake. We suggest therefore that a holistic view on the marine carbon cycle, including both organic matter production and consumption processes, is critical for assessing the efficacy of geoengineering tools that profoundly affect ecological systems. Most importantly, to draw a final conclusion on the potential impact of such CDR techniques, the current status of the nutrient limitation by phytoplankton and the heterotrophic microbial community must be known. However, the nature of the nutrient limitation that governs this balance is currently not fully understood. Once more knowledge on the iron limitation of heterotrophic bacteria is known, a more integrated evaluation would be to couple our MICDOC framework to a fully dynamic representation of iron cycling (Jürchott et al., 2024). Our results therefore call for dedicated experimental assessments of nutrient limitation and co-limitation of heterotrophic microbial communities, in a geographic context.

Code and data availability. The source code required to reproduce the model simulations, together with selected model outputs used to generate the figures in this manuscript, is available in the Zenodo repository at https://doi.org/10.5281/zenodo.23405565.

Author contributions. Benjamin Owusu and Sinikka Lennartz were responsible for the conceptualisation. Benjamin Owusu was responsible for data curation, formal analysis, methodology, software development, model simulations, validation, visualisation, and writing of the original draft. Wolfgang Koeve, Takasumi Kurahashi-Nakamura, Lennard Montag, and Sinikka T. Lennartz contributed to conceptualisation, methodology, software development, validation, and review and editing of the manuscript. The work was supervised by Sinikka T. Lennartz.

Competing interests. The authors declare no relevant conflict of interest in relation to this study.

Acknowledgements. We acknowledge funding from the Ministerium fuer Wissenschaft und Kultur Niedersachsen (MWK, Grant 16TTP079)

https://doi.org/10.5194/egusphere-2026-6818
Preprint. Discussion started: 6 November 2026
© Author(s) 2026. CC BY 4.0 License.

References

Adler, C., Wester, P., Bhatt, I., Huggel, C., Insarov, G., Morecroft, M., Muccione, V., and Prakash, A.: Cross-Chapter Paper 5: Mountains, pp. 2273–2318, Cambridge University Press, Cambridge, UK and New York, USA, ISBN 9781009325844, https://doi.org/10.1017/9781009325844.022.2273, 2022.

Azam, F., Smith, D., Steward, G., and Hagström, Å.: Bacteria-organic matter coupling and its significance for oceanic carbon cycling, Microbial ecology, 28, 167–179, 1994.

Baltar, F., Gutiérrez-Rodríguez, A., Meyer, M., Skudelny, I., Sander, S., Thomson, B., Nodder, S., Middag, R., and Morales, S. E.: Specific effect of trace metals on marine heterotrophic microbial activity and diversity: Key role of iron and zinc and hydrocarbon-degrading bacteria, Frontiers in Microbiology, 9, 3190, 2018.

Behrenfeld, M. J., Bale, A. J., Kolber, Z. S., Aiken, J., and Falkowski, P. G.: Confirmation of iron limitation of phytoplankton photosynthesis in the equatorial Pacific Ocean, Nature, 383, 508–511, 1996.

Bertrand, E. M., Saito, M. A., Lee, P. A., Dunbar, R. B., Sedwick, P. N., and DiTullio, G. R.: Iron limitation of a springtime bacterial and phytoplankton community in the Ross Sea: implications for vitamin B12 nutrition, Frontiers in Microbiology, 2, 160, 2011.

Boyd, P. W. and Vivian, C. M. G., eds.: High level review of a wide range of proposed marine geoengineering techniques, p. 144, no. 98 in Rep. Stud. GESAMP, International Maritime Organisation, London, iMO/FAO/UNESCO-IOC/UNIDO/WMO/IAEA/UN/UN Environment/UNDP/ISA Joint Group of Experts on the Scientific Aspect of Marine Environmental Protection, 2019.

Church, M. J., Hutchins, D. A., and Ducklow, H. W.: Limitation of bacterial growth by dissolved organic matter and iron in the Southern Ocean, Applied and Environmental Microbiology, 66, 455–466, 2000.

Currie, D. J. and Kalff, J.: Can bacteria outcompete phytoplankton for phosphorus? a chemostat test, Microbial Ecology, 10, 205–216, https://doi.org/10.1007/BF02010935, 1984.

Danovaro, R.: Do Bacteria Compete with Phytoplankton for Inorganic Nutrients? Possible Ecological Implications, Chemistry and Ecology, 14, 83–96, https://doi.org/10.1080/02757549808035544, 1998.

Dutreuil, S., Bopp, L., and Tagliabue, A.: Impact of enhanced vertical mixing on marine biogeochemistry: lessons for geo-engineering and natural variability, Biogeosciences, 6, 901–912, 2009.

Field, C. B., Behrenfeld, M. J., Randerson, J. T., and Falkowski, P.: Primary production of the biosphere: integrating terrestrial and oceanic components, science, 281, 237–240, 1998.

Fourquez, M., Devez, A., Schaumann, A., Gueneugues, A., Jouenne, T., Obernosterer, I., and Blain, S.: Effects of iron limitation on growth and carbon metabolism in oceanic and coastal heterotrophic bacteria, Limnology and oceanography, 59, 349–360, 2014.

Friedlingstein, P., O'sullivan, M., Jones, M. W., Andrew, R. M., Hauck, J., Landschützer, P., Le Quéré, C., Li, H., Luijkx, I. T., Olsen, A., et al.: Global carbon budget 2024, Earth System Science Data Discussions, 2024, 1–133, 2024.

Galbraith, E. D., Gnanadesikan, A., Dunne, J. P., and Hiscock, M. R.: Regional impacts of iron-light colimitation in a global biogeochemical model, Biogeosciences, 7, 1043–1064, 2010.

Garcia, H. E. and Gordon, L. I.: Oxygen solubility in seawater: Better fitting equations, Limnology and Oceanography, 37, 1307–1312, https://doi.org/https://doi.org/10.4319/lo.1992.37.6.1307, 1992.

Garcia, H. E., Weathers, K. W., Paver, C. R., Smolyar, I., Boyer, T. P., Locarnini, M. M., Zweng, M. M., Mishonov, A. V., Baranova, O. K., Seidov, D., and Reagan, J. R.: World Ocean Atlas 2018. Vol. 4: Dissolved Inorganic Nutrients (phosphate, nitrate and nitrate+nitrite, silicate), Tech. rep., NOAA Atlas NESDIS 84, https://archimer.ifremer.fr/doc/00651/76336/, a. Mishonov, Technical Editor, 2019.

https://doi.org/10.5194/egusphere-2026-6818
Preprint. Discussion started: 6 November 2026
© Author(s) 2026. CC BY 4.0 License.

Geider, R. J. and La Roche, J.: The role of iron in phytoplankton photosynthesis, and the potential for iron-limitation of primary productivity in the sea, Photosynthesis research, 39, 275–301, 1994.

Gidden, M. J., Riahi, K., Smith, S. J., Fujimori, S., Luderer, G., Kriegler, E., van Vuuren, D. P., van den Berg, M., Feng, L., Klein, D., Calvin, K., Doelman, J. C., Frank, S., Fricko, O., Harmsen, M., Hasegawa, T., Havlik, P., Hilaire, J., Hoesly, R., Horing, J., Popp, A., Stehfest, E., and Takahashi, K.: Global emissions pathways under different socioeconomic scenarios for use in CMIP6: a dataset of harmonized emissions trajectories through the end of the century, Geoscientific Model Development, 12, 1443–1475, https://doi.org/10.5194/gmd-12-1443-2019, 2019.

Gomez-Letona, M., Sebastian, M., Baños, I., Montero, M. F., Barrancos, C. P., Baumann, M., Riebesell, U., and Aristegui, J.: The importance of the dissolved organic matter pool for the carbon sequestration potential of artificial upwelling, Frontiers in Marine Science, 9, 969 714, 2022.

Grognard, F., Masci, P., Benoît, E., and Bernard, O.: Competition between phytoplankton and bacteria: exclusion and coexistence, Journal of Mathematical Biology, 70, 959–1006, 2015.

Hale, M. S., Li, W. K., and Rivkin, R. B.: Meridional patterns of inorganic nutrient limitation and co-limitation of bacterial growth in the Atlantic Ocean, Progress in Oceanography, 158, 90–98, https://doi.org/10.1016/j.pocean.2016.11.007, 2017.

Hansell, D. A.: Dissolved organic carbon in the carbon cycle of the Indian Ocean, Indian Ocean biogeochemical processes and ecological variability, 185, 217–230, 2009.

Hansell, D. A. and Carlson, C. A.: Marine dissolved organic matter and the carbon cycle, Oceanography, 14, 41–49, 2001.

Hansell, D. A., Carlson, C. A., Amon, R. M., Álvarez-Salgado, X. A., Yamashita, Y., Romera-Castillo, C., and Bif, M. B.: Compilation of dissolved organic matter (DOM) data obtained from the global ocean surveys from 1994 to 2020 (NCEI Accession 0227166), NOAA National Centers for Environmental Information. Dataset. DOI: https://doi. org/10.25921/s4f4-ye35. Accessed [date], 2021.

Hao, J., Sun, Y., Shang, X., Wang, B., Huang, H., Wang, A., Yang, X., Jia, L., and Sun, J.: Harnessing the microbial carbon pump: prospects and challenges for coastal carbon sequestration, Frontiers in Marine Science, 2026.

Holland-Cunz, A. and Baatz, C.: How to govern carbon dioxide removal: an assessment framework for policy instruments, Climate Policy, pp. 1–16, 2025.

Honegger, M., Baatz, C., Eberenz, S., Holland-Cunz, A., Michaelowa, A., Pokorny, B., Poralla, M., and Winkler, M.: The ABC of governance principles for carbon dioxide removal policy, Frontiers in Climate, 4, 884 163, 2022.

Hopkinson Jr, C. S. and Vallino, J. J.: Efficient export of carbon to the deep ocean through dissolved organic matter, Nature, 433, 142–145, 2005.

Hurrell, J. W., Haywood, J. M., Lawrence, P. J., Lennard, C. J., and Oschlies, A.: Climate intervention research in the world climate research Programme: a perspective, Frontiers in Climate, 6, 1505 860, 2024.

Jiao, N. and Azam, F.: Microbial carbon pump and its significance for carbon sequestration in the ocean, Microbial carbon pump in the ocean, 10, 43–45, 2011.

Joint, I., Henriksen, P., Flaten, G. A., Bourne, D., Thingstad, T., and Riemann, B.: Competition for inorganic nutrients between phytoplankton and bacterioplankton in nutrient manipulated mesocosms, Aquatic Microbial Ecology, 29, 145–159, https://doi.org/10.3354/ame029145, 2002.

Jürchott, M., Oschlies, A., and Koeve, W.: Artificial upwelling – A refined narrative, Geophysical Research Letters, 50, e2022GL101 870, 2023.

https://doi.org/10.5194/egusphere-2026-6818
Preprint. Discussion started: 6 November 2026
© Author(s) 2026. CC BY 4.0 License.

Jürchott, M., Koeve, W., and Oschlies, A.: The response of the ocean carbon cycle to artificial upwelling, ocean iron fertilization and the combination of both, Environmental Research Letters, 19, 114 088, 2024.

Keller, D. P., Oschlies, A., and Eby, M.: A new marine ecosystem model for the University of Victoria Earth System Climate Model, Geoscientific Model Development, 5, 1195–1220, 2012.

Keller, D. P., Feng, E. Y., and Oschlies, A.: Potential climate engineering effectiveness and side effects during a high carbon dioxide-emission scenario, Nature communications, 5, 3304, 2014.

Kikstra, J. S., Nicholls, Z. R., Smith, C. J., Lewis, J., Lamboll, R. D., Byers, E., Sandstad, M., Meinshausen, M., Gidden, M. J., Rogelj, J., et al.: The IPCC Sixth Assessment Report WGIII climate assessment of mitigation pathways: from emissions to global temperatures, Geoscientific Model Development, 15, 9075–9109, 2022.

Kirchman, D. L., Hoffman, K. A., Weaver, R., and Hutchins, D. A.: Regulation of growth and energetics of a marine bacterium by nitrogen source and iron availability, Marine Ecology Progress Series, 250, 291–296, 2003.

Kurahashi-Nakamura, T., Dittmar, T., Martiny, A. C., and Lennartz, S. T.: Enhanced carbon storage in dissolved organic matter in a future oligotrophic ocean, bioRxiv, https://doi.org/https://doi.org/10.64898/2026.04.02.71603, 2026.

Lee, H., Calvin, K., Dasgupta, D., Krinner, G., Mukherji, A., Thorne, P., Trisos, C., Romero, J., Aldunce, P., Barret, K., et al.: IPCC, 2023: Climate change 2023: Synthesis report, summary for policymakers. Contribution of working groups i, II and III to the sixth assessment report of the intergovernmental panel on climate change [core writing team, h. Lee and j. Romero (eds.)]. IPCC, geneva, Switzerland., Tech. rep., Intergovernmental Panel on Climate Change (IPCC), 2023.

Lennartz, S. T., Keller, D. P., Oschlies, A., Blasius, B., and Dittmar, T.: Mechanisms underpinning the net removal rates of dissolved organic carbon in the global ocean, Global Biogeochemical Cycles, 38, e2023GB007 912, 2024.

Lévy, M., Bopp, L., Karleskind, P., Resplandy, L., Éthé, C., and Pinsard, F.: Physical pathways for carbon transfers between the surface mixed layer and the ocean interior, Global Biogeochemical Cycles, 27, 1001–1012, 2013.

Locarnini, M. M., Mishonov, A. V., Baranova, O. K., Boyer, T. P., Zweng, M. M., Garcia, H. E., Reagan, J. R., Seidov, D., Weathers, K. W., Paver, C. R., and Smolyar, I.: World Ocean Atlas 2018, Volume 1: Temperature, Tech. Rep. 81, NOAA National Centers for Environmental Information, https://archimer.ifremer.fr/doc/00651/76338/, a. Mishonov, Technical Editor, 2018.

Mace, M., Fyson, C. L., Schaeffer, M., and Hare, W. L.: Large-scale carbon dioxide removal to meet the 1.5 C limit: key governance gaps, challenges and priority responses, Global Policy, 12, 67–81, 2021.

Mellett, T., Monreal, P., Kunde, K., Manck, L. E., Cain, K., Ribalet, F., Church, M. J., Armbrust, E. V., and Bundy, R. M.: Iron availability modulates bacteria carbon cycling in the mesopelagic, Scientific Reports, 2026.

Mengis, N., Keller, D. P., MacDougall, A. H., Eby, M., Wright, N., Meissner, K. J., Oschlies, A., Schmittner, A., MacIsaac, A. J., Matthews, H. D., et al.: Evaluation of the University of Victoria earth system climate model version 2.10 (UVic ESCM 2.10), Geoscientific Model Development, 13, 4183–4204, 2020.

Mentges, A., Deutsch, C., Feenders, C., Lennartz, S. T., Blasius, B., and Dittmar, T.: Microbial physiology governs the oceanic distribution of dissolved organic carbon in a scenario of equal degradability, Frontiers in Marine Science, 7, 549 784, 2020.

Oschlies, A., Pahlow, M., Yool, A., and Matear, R. J.: Climate engineering by artificial ocean upwelling: Channelling the sorcerer's apprentice, Geophysical Research Letters, 37, 2010.

Owusu, B., Lücken, L., Kurahashi-Nakamura, T., and Lennartz, S. T.: Dissolved organic carbon accumulation in the North Atlantic subtropical gyre: Microbial feedbacks and ecological controls along Lagrangian trajectories, Journal of Geophysical Research: Biogeosciences, 131, e2025JG009 257, https://doi.org/10.1029/2025JG009257, 2026.

https://doi.org/10.5194/egusphere-2026-6818
Preprint. Discussion started: 6 November 2026
© Author(s) 2026. CC BY 4.0 License.

Pan, Y., Fan, W., Zhang, D., Chen, J., Huang, H., Liu, S., Jiang, Z., Di, Y., Tong, M., and Chen, Y.: Research progress in artificial upwelling and its potential environmental effects, Science China Earth Sciences, 59, 236–248, 2016.

Parekh, P., Follows, M. J., and Boyle, E.: Modeling the global ocean iron cycle, Global biogeochemical cycles, 18, 2004.

Pham, A. L.-D., Aumont, O., Ratnarajah, L., and Tagliabue, A.: Examining the interaction between free-living bacteria and iron in the global ocean, Global Biogeochemical Cycles, 36, e2021GB007 194, 2022.

Polimene, L., Allen, J., and Zavatarelli, M.: Model of interactions between dissolved organic carbon and bacteria in marine systems, Aquatic microbial ecology, 43, 127–138, 2006.

Sarmiento, J. and Gruber, N.: Ocean Biogeochemical Dynamics. xiii+ 503 pp. Princeton, Woodstock: Princeton University Press. Price£ 48.95 (hard covers). 0 691 01707 7., Geological Magazine, 144, 1034–1034, 2006.

Schmittner, A., Oschlies, A., Matthews, H. D., and Galbraith, E. D.: Future changes in climate, ocean circulation, ecosystems, and biogeochemical cycling simulated for a business-as-usual CO2 emission scenario until year 4000 AD, Global biogeochemical cycles, 22, 2008.

Shepherd, J., Iglesias-Rodriguez, D., and Yool, A.: Geo-engineering might cause, not cure, problems, Nature, 449, 781–781, 2007.

Singh, S. K., Kotakonda, A., Kapardar, R. K., Kankipati, H. K., Sreenivasa Rao, P., Sankaranarayanan, P. M., Vetaikorumagan, S. R., Gundlapally, S. R., Nagappa, R., and Shivaji, S.: Response of bacterioplankton to iron fertilization of the Southern Ocean, Antarctica, Frontiers in Microbiology, 6, 863, 2015.

Sörenson, E., Farnelid, H., Lindehoff, E., and Legrand, C.: Resource partitioning between phytoplankton and bacteria in the coastal Baltic Sea, Frontiers in Marine Science, 7, 608 244, 2020.

Tang, J. and Riley, W. J.: Finding Liebig's law of the minimum, Ecological Applications, 31, e02 458, 2021.

Van Vuuren, D. P., O'Neill, B. C., Tebaldi, C., Sanderson, B. M., Chini, L. P., Friedlingstein, P., Hasegawa, T., Riahi, K., Govindasamy, B., Bauer, N., et al.: The scenario model intercomparison project for CMIP7 (ScenarioMIP-CMIP7), Geoscientific Model Development, 19, 2627–2656, 2026.

Volk, T. and Hoffert, M. I.: Ocean carbon pumps: Analysis of relative strengths and efficiencies in ocean-driven atmospheric CO2 changes, The carbon cycle and atmospheric CO2: Natural variations Archean to present, 32, 99–110, 1985.

Weaver, A. J., Eby, M., Wiebe, E. C., Bitz, C. M., Duffy, P. B., Ewen, T. L., Fanning, A. F., Holland, M. M., MacFadyen, A., Matthews, H. D., et al.: The UVic Earth System Climate Model: Model description, climatology, and applications to past, present and future climates, Atmosphere-ocean, 39, 361–428, 2001.

Yool, A., Shepherd, J. G., Bryden, H. L., and Oschlies, A.: Low efficiency of nutrient translocation for enhancing oceanic uptake of carbon dioxide, Journal of Geophysical Research: Oceans, 114, 2009.

Zakem, E. J. and Levine, N. M.: Systematic variation in marine dissolved organic matter stoichiometry and remineralization ratios as a function of lability, Global Biogeochemical Cycles, 33, 1389–1407, 2019.

Zweifel, U. L., Norrman, B., and Hagstrom, A.: Consumption of dissolved organic carbon by marine bacteria and demand for inorganic nutrients, Marine Ecology Progress Series, 101, 23–32, 1993.